ELSEVIER

Journal of Photochemistry and Photobiology A: Chemistry 155 (2003) 171–178

Journal of Photochemistry and Photobiology A:Chemistry

www.elsevier.com/locate/jphotochem

Synthesis of nitrogen-containing ZnO powders by spray pyrolysis and their visible-light photocatalysis in gas-phase acetaldehyde decomposition

Di Li, Hajime Haneda*

Advanced Materials Laboratory, National Institute for Materials Science (NIMS), 1-1 Namiki, Tsukuba 305-0047, Japan

Received 17 June 2002; received in revised form 13 September 2002; accepted 5 October 2002

Abstract

Colored N-containing ZnO powders with high surface area were synthesized by spray pyrolysis. The total nitrogen concentration was controlled from 600 to 1400 ppm by changing the pyrolysis temperature. The concentration of nitrogen doped into the sites of the ZnO crystal lattice by replacing oxygen atoms ranged from 400 to 900 ppm. Ultraviolet-visible spectra indicated that the N-containing ZnO powders could absorb not only ultraviolet light ($\lambda < 387$ nm) like pure ZnO powder, but also part of the visible light ($\lambda < 650$ nm). Acetaldehyde decomposition was used as a probe reaction to evaluate the photocatalysis of these N-containing ZnO powders. The photocatalytic performance of the sprayed N-containing ZnO powder was superior to that of a pure ZnO sample under visible light irradiation. However, nitrogen introduction did not remarkably improve the UV photocatalytic activity of ZnO.

Keywords: Nitrogen-doping; Zinc oxide; Spray pyrolysis; Photocatalysis; Acetaldehyde

1. Introduction

As a well-known photocatalyst, ZnO has received much attention with respect to the degradation of various environmental pollutants [1–3]. However, these photocatalytic transformations only proceed under UV irradiation because ZnO is a semiconductor with a wide band-gap of about 3.2 eV and can only absorb UV light with $\lambda < 387$ nm. Therefore, a material capable of visible-light photocatalysis is required with regard to solar energy and interior lighting applications. Changing the optical absorption properties, i.e. narrowing the band-gap, will be necessary to attain this goal. One successful approach has been to implant transition metal ions, e.g. V, or Cr ions, into a TiO_2 powder or film [4,5]. However, an expensive ion-implantation facility is needed for this process. Recent research has shown that N-doping into the substitutional sites of TiO_2, Ta_2O_5, or $LaTaO_4$ by calcination in an NH_3 or N_2 atmosphere is effective for band-gap narrowing and visible-light photocatalysis [6–8]. Similar results are also expected for ZnO since it has almost the same band-gap energy as TiO_2.

Recently, Futsuhara et al. synthesized zinc oxynitride ($Zn_xO_yN_z$) thin films from a ZnO target in N_2–Ar mixtures by reactive rf magnetron sputtering and found that the optical band-gap decreased from 3.26 to 2.30 eV when the nitrogen concentration in films increased from 0 to 10 at.% [9]. This corresponds to an absorption edge shift from 380 to 539 nm. Additionally, a visible-light absorption feature was also observed on N-doped ZnO thin films [10]. These results indicate that the substitution of some of the oxygen atoms with nitrogen atoms in a ZnO crystal lattice can significantly improve the optical absorption properties of ZnO. However, these studies were focused on thin film samples and their photocatalysis was not investigated. In our work, N-containing ZnO powders, instead of thin films, were prepared by spray pyrolysis. As far as we know, there have been no other reports on the synthesis and photocatalysis of N-containing ZnO powders.

A common synthesis route for N-doped metal oxide powder is the reaction of the metal oxide with flowing ammonia gas at elevated temperatures [6–8]. However, the surface area of the N-doped metal oxide powder obtained by this method is much less than that of the original metal oxide since a high temperature is required to introduce nitrogen atoms into the metal oxide crystal lattice.

Spray pyrolysis is a versatile technique for producing ceramic materials with a wide variety of particle morphologies,

* Corresponding author. Tel.: +81-298-51-3354x575; fax: +81-298-55-1196.
E-mail address: haneda.hajime@nims.go.jp (H. Haneda).

1010-6030/02/$ – see front matter © 2002 Elsevier Science B.V. All rights reserved.
PII: S1010-6030(02)00371-4

sizes and compositions [11,12]. It has also been used to prepare thermocatalysts and photocatalysts, and these catalysts demonstrated better performances than those prepared by conventional impregnation [13–15]. A distinctive feature of sprayed catalysts is the homogeneous distribution of the ingredients throughout the entire particle since all ingredients are formed from a homogeneous solution. With this advantage, we expected that nitrogen atoms could be introduced into a ZnO crystal lattice and that the distribution of the nitrogen atoms would be homogeneous throughout the crystallite.

In this paper, we describe our synthesis by spray pyrolysis of a series of N-containing ZnO powders with different nitrogen concentrations. We used scanning electron microscopy (SEM), elemental analysis, thermogravimetric and differential thermal analysis (TG-DTA), X-ray diffraction (XRD), and ultraviolet-visible (UV-Vis) diffuse reflectance spectroscopy to characterize these N-containing ZnO powders. Acetaldehyde photodecomposition was used as a probe reaction to evaluate their photocatalysis. The relationship between the characteristics of the N-containing ZnO powders and their photocatalysis is discussed.

2. Experimental

2.1. Synthesis of N-containing ZnO powders by spray pyrolysis

High purity ZnO (High Purity Chemicals, Japan, 99.999%) was used as a zinc source. First, the ZnO was dissolved in an appropriate ammonia aqueous solution to obtain a 0.1 M zinc-ammonia complex solution. The zinc–ammonia solution was then atomized by a nebulizer and passed through a high-temperature quartz tube under the suction of an aspirator. The pyrolysis proceeded quickly as droplets passed through the high-temperature tube within a second. The formed N-containing ZnO powder was collected with a glass filter, which was installed at the end of the tube. A series of N-containing ZnO powders were prepared by changing the pyrolysis temperature, and these were designated as spr-400, spr-600, spr-800, and spr-1000. Here, the numbers indicate the pyrolysis temperature in degree Celsius.

For comparison, we also measured the photocatalytic performance of commercial ZnO (Sakai Chemical Industry Co. Ltd., Nanofine P-2) with a BET surface area of $50\,m^2\,g^{-1}$. This ZnO was denoted as com-ZnO.

2.2. Characterization

The particle morphology was observed with a JEOL S-5000 scanning electron microscope (SEM) using an acceleration voltage of 10 kV. XRD patterns were recorded on a Philips PW1800 X-ray diffractometer with Cu Kα radiation. Ultraviolet-visible diffuse reflectance spectra were obtained on a JASCO V-550 spectrophotometer. Thermogravimetric and differential thermal analysis (TG-DTA) was performed on a TG/DTA6200 system (Seiko Instruments Inc.) in an air atmosphere. Samples were heated from room temperature to 1073 K at $10\,K\,min^{-1}$. The BET surface area of ZnO sample was determined by N_2 adsorption and desorption at 77 K in a model 4201 automatic surface area analyzer (Beta Scientific Corp.). Nitrogen elemental analysis was done with a nitrogen/oxygen determinator (LECO Corporation, USA, TC-436) by heating the sample in inert gas then using a thermal conductivity detector to analyze the obtained nitrogen.

2.3. Photocatalytic system

Photocatalytic decomposition of acetaldehyde was carried out in a closed circulation system ($250\,cm^3$) interfaced to a gas chromatograph (Hitachi G-35A) with a TCD and a PID detector for CH_3CHO and CO_2 analysis, respectively. Prior to the catalytic experiments, the ZnO samples (0.0500 g) were outgassed under a vacuum of 10^{-5} Pa at 398 K for 2.0 h. A gas mixture of 88.0 kPa CH_3CHO–He (730 ppm) and 13.3 kPa O_2 was then introduced. The samples were irradiated from the outside of the reactor. A 200 W Hg–Xe lamp (LA-300UV, $\lambda_{max} = 365$ nm) and a 150 W Xe lamp (LA-254Xe, $\lambda_{max} = 470$ nm, Hayashi Watch-Works. Co. Ltd., Japan) were used as UV and visible light sources, respectively. The wavelength of the visible light was controlled through an L-39 390 nm cut filter or an L-42 420 nm cut filter (Kenko, Japan). The incident intensity of the sample surface for both light sources was set up to be $20\,mW\,cm^{-2}$.

3. Results and discussion

3.1. Characterization of N-containing ZnO powders

3.1.1. Morphology

Four kinds of N-containing ZnO powders were synthesized by spray pyrolysis at different temperatures. These powders were strongly orange in color, with the shades of color depending on the pyrolysis temperatures. SEM images of spr-400 and spr-800 are shown in Fig. 1. Particles with open, microscopic surface porosity were observed in both samples. The particulate morphology slightly depended on the pyrolysis temperature. However, an obvious difference appeared on the wall of the spherical particles. The surface of the spr-400 particles was smooth (Fig. 1b), whereas the surface of the spr-800 particles was rough and consisted of visibly primary particles (Fig. 1d). This indicates that a higher pyrolysis temperature facilitates the growth of primary particles. The morphologies of the spr-600 and spr-1000 samples were similar to those of the spr-400 and spr-800 samples, respectively.

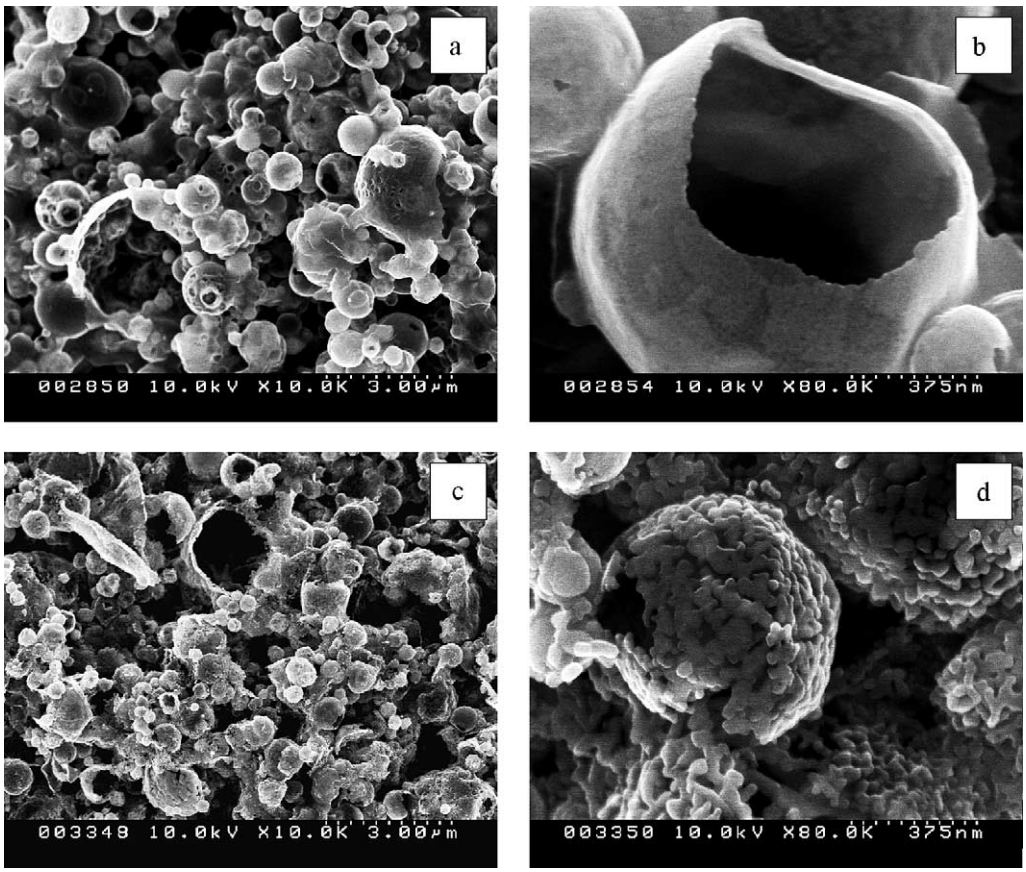

Fig. 1. SEM images of spr-400 (a, b) and spr-800 (c, d).

3.1.2. Chemical composition

The chemical composition of the as-sprayed powders was determined by elemental analysis. The results, as well as the BET surface area, are listed in Table 1. The nitrogen concentration greatly depended on the pyrolysis temperature and ranged from 600 to 1400 ppm. The BET value fell from 59 to 33 $m^2 g^{-1}$ as the pyrolysis temperature rose from 673 to 1273 K. However, the value for spr-400 exceeded that of nanofine com-ZnO (50 $m^2 g^{-1}$), which is generally regarded as the commercial ZnO powder with the highest BET surface area. This result indicates that spray pyrolysis should be an excellent and practical method for preparing N-containing powders with high surface area.

3.1.3. Structure

XRD patterns of the N-containing ZnO powders are shown in Fig. 2. All diffraction peaks could be identified as ZnO peaks and no Zn_3N_2 peaks were observed. This suggests that the introduction of nitrogen atoms does not change the ZnO crystal structure. Additionally, a clear sharpening and attenuation of the peaks can be observed as the pyrolysis temperature rose, but there was no noticeable change in the intensity ratios between the peaks. The crystallite sizes obtained from the 102 peak of the XRD pattern for the N-containing ZnO powders were 12.8, 25.2, 41.2,

Table 1
Elemental analysis of as-sprayed N-containing ZnO powders

Sample	Zn (wt.%)	O (wt.%)	N (wt.%)	H_2O (wt.%)	BET ($m^2 g^{-1}$)
Spr-400	76.3	22.7	0.14	3.2	59
Spr-600	78.3	21.0	0.11	1.8	50
Spr-800	79.4	20.5	0.09	0.7	39
Spr-1000	79.7	20.3	0.06	0.7	33
Com-ZnO	79.1	19.5	<0.01	1.0	50

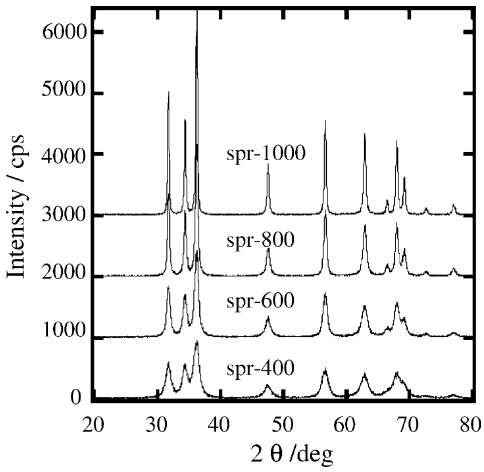

Fig. 2. XRD patterns of N-containing ZnO powders.

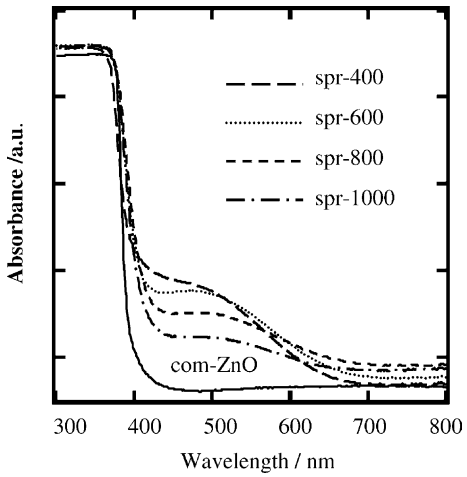

Fig. 3. UV-Vis adsorption spectra of N-containing ZnO powders.

and 56.8 nm for spr-400, spr-600, spr-800, and spr-1000, respectively. The crystallite size for spr-800 agreed with that of the observed primary particles (Fig. 1d).

3.1.4. Optical property

Fig. 3 shows the absorption spectra of the N-containing ZnO powders and a commercial ZnO powder for comparison. The spectral pattern depended on the pyrolysis temperature. Two absorption edges were observed for all the N-containing ZnO powders. One edge was in the UV range at about 385 nm for all samples except spr-400, and was regarded as the fundamental absorption edge of ZnO. The poor crystallinity of spr-400 (Fig. 2) caused its UV absorption edge to shift to about 375 nm. Therefore, nitrogen introduction did not remarkably affect this absorption edge. The other absorption edge was in the visible range at about 500 nm, corresponding to a band-gap of about 2.5 eV, and changed slightly with the pyrolysis temperature. This result is consistent with that observed for a zinc oxynitride ($Zn_xO_yN_z$) thin film [9], confirming that at least some of the nitrogen atoms in the N-containing ZnO powders existed in the same chemical state as in zinc oxynitride, i.e. nitrogen atoms were doped into the oxygen sites of the ZnO crystal lattice. The decrease of the energy-gap accounts for the difference in the energy levels of the oxygen and nitrogen 2p orbitals: $E_{2p}(O) = -14.8$ eV and $E_{2p}(N) = -13.4$ eV [16,17].

3.1.5. Thermal behavior

To understand the stability of nitrogen, we investigated the thermal behavior of as-sprayed powders. TG-DTA curves for spr-400 and spr-800 are shown in Fig. 4. A clear exothermic reaction peak at about 773 K was observed. We assigned this reaction to the decomposition of ZnO precursor ($Zn(NH_3)_4(OH)_2$) residues since such a peak was not found for com-ZnO. The weight losses of spr-400 and spr-800 near 773 K were 0.075 and 0.036%, respectively, indicating that the residual amount of the ZnO precursor decreased with the pyrolysis temperature. This weight loss

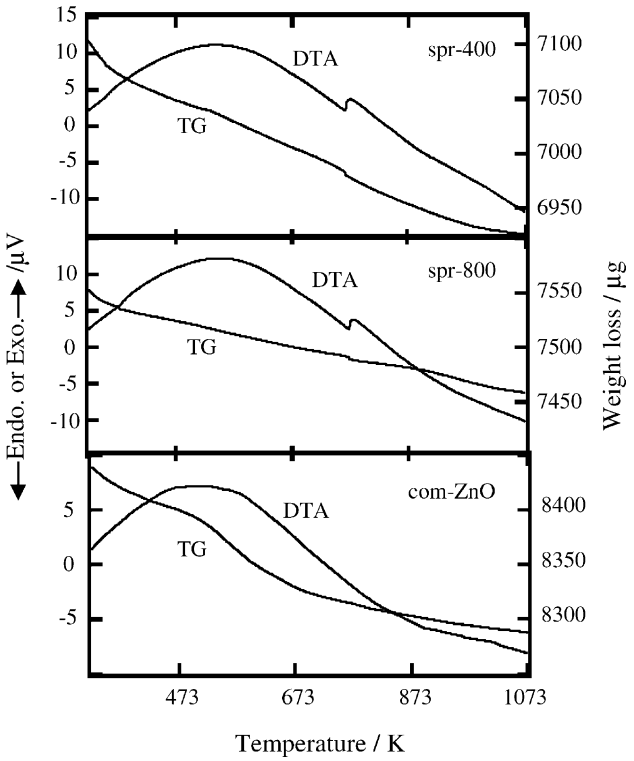

Fig. 4. TG-DTA curves of spr-400 and spr-800.

corresponded to 0.19% $Zn(NH_3)_4(OH)_2$ content in spr-400 and 0.069% in spr-800 since the weight loss would be 51.5% if $Zn(NH_3)_4(OH)_2$ completely decomposed into ZnO. This also shows that 630 ppm nitrogen in spr-400 and 230 ppm nitrogen in spr-800 have been present in the form of the ZnO precursor or an intermediate from the incomplete decomposition of $Zn(NH_3)_4(OH)_2$. In this study, we call this nitrogen component 'residue-N'. Obviously, the residue-N atoms were not introduced into the sites of the ZnO crystal lattice. Similar TG-DTA curves were also obtained for spr-600 and spr-1000, which corresponded to residue-N of 280 and 210 ppm, respectively.

3.1.6. Chemical forms of nitrogen in sprayed ZnO powders

Based on the UV-Vis spectra and TG-DTA curves, we concluded that the nitrogen atoms in the sprayed ZnO powder existed in two chemical forms. One is the residue-N that originated from the ZnO precursor residues. The other is the nitrogen atoms that were doped into the ZnO crystal lattice by replacing oxygen atoms. Here, we called these nitrogen atoms 'site-N'. Although additional experimental evidence, except the optical absorption spectra, is needed to support this conclusion, two facts indirectly prove the existence of nitrogen/oxygen substitution. The first is that the N-containing ZnO powders were strongly colored. In general, the color is determined by the position of the absorption edge whose shift towards a higher wavelength can result in absorption in the visible part of the spectrum; this shift of the absorption edge should be ascribed to the substitutional doping of nitro-

Table 2
Chemical forms and concentrations of nitrogen in the N-containing ZnO powders

Sample	Spr-400 (ppm)	Spr-600 (ppm)	Spr-800 (ppm)	Spr-1000 (ppm)
Total nitrogen	1400	1100	900	600
Residue-N	630[a] (700[b])	280 (200)	230 (300)	210 (200)
Site-N	770 (700)	820 (900)	670 (600)	390 (400)
x ($ZnO_{1-x}N_x$)	0.0041[c]	0.0052	0.0035	0.0023

[a] From the TG-DTA data.
[b] From the elemental analysis of the sample calcined in air atmosphere at 873 K for 2 h.
[c] Calculated from the elemental analysis data.

gen atoms as in nitride-type compounds [8,17]. The second fact is that the N-containing ZnO powder was still colored even after calcination at 1073 K, indicating that some of the nitrogen atoms were very stable. This characteristic is also consistent with that of the site-N in ZnO single crystals [18].

Based on the residue-N concentration obtained from our TG-DTA data, we calculated the site-N concentration by subtracting the residue-N content from the total nitrogen content (Table 1). The results are listed in Table 2.

Additionally, we also estimate the site-N concentration through an elemental analysis of the N-containing powders calcined in air atmosphere at 873 K for 2.0 h. The nitrogen remaining in a sample after calcination was considered to be site-N. The lost portion of the nitrogen, the difference in a sample's nitrogen concentration before and after calcination, was considered the residue-N. The site-N and residue-N concentrations in each calcined sample are also summarized in Table 2. The site-N concentration from the elemental analysis of each sample agrees with the result from the TG-DTA data.

3.2. Photocatalysis of N-containing ZnO powders

3.2.1. Photocatalytic activity under UV irradiation

The effects of nitrogen introduction on the UV photocatalysis of ZnO powders were investigated and shown in Fig. 5. No significant difference in CO_2 concentration after 2 h of UV irradiation was observed between the N-containing ZnO powder and the pure com-ZnO or among the N-containing ZnO powders. This suggests that nitrogen introduction did not significantly affect the UV photocatalysis of the ZnO powders. Nevertheless, it should be noted that the CO_2 concentration increased exponentially with the photo-irradiation time over spr-400, but increased linearly over spr-1000; this distinctive difference in the shape of the CO_2 concentration–time curves probably means that the acetaldehyde decomposition occurred through different reaction mechanisms [19,20]. This result is probably closely related to the obvious change in the particle surface with the pyrolysis temperature (Fig. 1).

The initial rate of N-containing ZnO powders was calculated for the initial 30 min photo-irradiation time and shown in Fig. 6. It decreased monotonically with increasing pyrolysis temperature. We ascribe this to two factors. One is

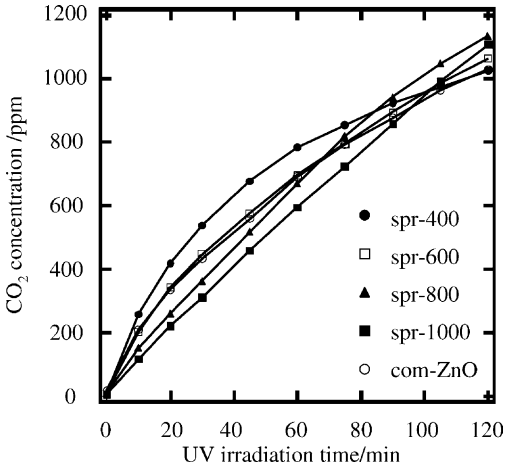

Fig. 5. Time-course of the CO_2 evolution during UV photocatalytic decomposition of acetaldehyde on N-containing ZnO powders.

the great change in the morphologies of the particle surface (Fig. 1) with the pyrolysis temperature. This would result in the decrease not only in the BET surface area (Table 1) but also in the surface hydroxyl. The rapid decrease of water content in the sprayed ZnO powder as the pyrolysis temperature rose is indirect evidence supporting this speculation. Photodecomposition processes, in general, occur through

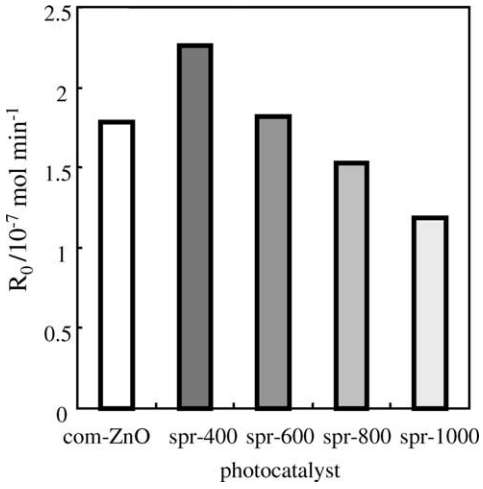

Fig. 6. Initial rates of the CO_2 evolution on N-containing ZnO powders for the UV photocatalytic decomposition of acetaldehyde.

the attack of organic substrates by activated species (e.g. OH radicals), and these activated species are generated via hole capture by the surface hydroxyl [20,21]. Therefore, we attributed the decrease in photocatalytic activity of the N-containing ZnO powders with pyrolysis temperature to a decrease in the surface hydroxyl. The second factor is the decrease of surface oxygen deficiencies with the pyrolysis temperature. Jing et al. found that the EPR signal intensity assigned to oxygen deficiencies rapidly decreased as the calcination temperature for ZnO ultrafine particles increased from 593 to 973 K [22]. Oxygen deficiencies can act as capture centers for photo-generated electrons, and thus, effectively restrain the recombination of electrons and holes. This will lead to improved photocatalysis. Our N-containing ZnO powders, especially when a low pyrolysis temperature was used, should have had more oxygen deficiencies since our pyrolysis lasted for less than a second.

In addition, the highest initial rate was that of spr-400. This is consistent with the reasons mentioned above. However, the higher residue-N concentration seems to be an additive factor since Markham's studies have indicated that hydroxylamine produces radicals under UV irradiation, and these radicals can accelerate the decomposition of a surface-adsorbed fragment [23].

The quantum yield for CO_2 formation on each sample, 1.0 h after the reaction started, was also calculated. It was 2.8% for spr-400, 2.5% for spr-600, 2.4% for spr-800, 2.1% for spr-1000, and 2.5% for com-ZnO. The com-ZnO and spr-600, which had the same BET surface area, also had the same initial rate and quantum yield, further demonstrating that the nitrogen introduction had little effect on the UV photocatalysis of ZnO powders.

3.2.2. Photocatalytic activity under visible light irradiation

As mentioned in the experimental section, the wavelength of the visible light (Vis) was controlled through a 390 nm or a 420 nm cut filter.

The effect of nitrogen introduction on the photocatalysis of the ZnO powders under Vis irradiation of more than 390 nm is shown in Fig. 7. The photocatalytic activity of each N-containing ZnO powder was much higher than that of the pure com-ZnO, indicating that the Vis photocatalysis of the ZnO powders was greatly improved by the nitrogen introduction. Moreover, the photocatalytic activities of N-containing ZnO powders depend significantly on the pyrolysis temperature. If the CO_2 concentration formed 6 h after the reaction began is used to represent the photocatalytic activity, the activity decreased in the order: spr-600 > spr-400 > spr-800 > spr-1000. This order is consistent with the site-N concentration in the samples, confirming that substitutional doping of nitrogen/oxygen atoms is an effective means of improving the visible-light photocatalysis of ZnO.

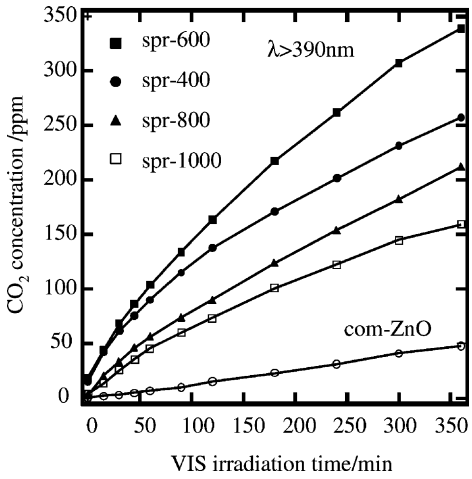

Fig. 7. Time-course of the CO_2 evolution during the Vis (>390 nm) photocatalytic decomposition of acetaldehyde on N-containing ZnO powders.

With regard to the Vis photocatalytic activity, we also calculated the initial rate of CO_2 formation, the CO_2 yield, and the quantum yield, 6 h after the reaction began through the time-course curve of CO_2 evolution. They are listed in Table 3. All activity parameters indicate that the maximum photocatalytic activity was that of spr-600 rather than spr-400 (as was the case under UV irradiation). This might be related to the UV absorption edge shift of spr-400 except for its site-N concentration.

The photocatalytic activities of N-containing ZnO powders under Vis irradiation of more than 420 nm are shown in Fig. 8. The results are similar to those for the 390 nm case.

The Vis photocatalysis of ZnO powder was significantly improved by a small amount of N-doping. We ascribe the improvement mechanism to a defect energy state, newly formed by N-doping between the valence (VB) and the conduction (CB) bands in the ZnO band structure. Fig. 9 illustrates our proposed energy-band structure in a N-doping ZnO photocatalyst. The electrons, generated in the VB from the Vis irradiation ($h\nu > 2.5$ eV), can first transfer to the defect energy state, and then further transfer to the CB by absorbing less energy ($h\nu > 0.8$ eV) than that of the first step transition. This means that the electron transition from VB to CB in ZnO semiconductor, generally produced by

Table 3
Visible light (>390 nm) photocatalytic properties of the N-containing ZnO powders

Photocatalytic activity	Spr-400	Spr-600	Spr-800	Spr-1000	Com-ZnO
CO_2 yield (%)	20.3	26.7	17.0	12.6	3.7
R_0 (10^{-8} mol min^{-1})	1.1	1.5	0.74	0.62	0.15
Quantum yield (%)	0.32	0.42	0.27	0.20	0.06

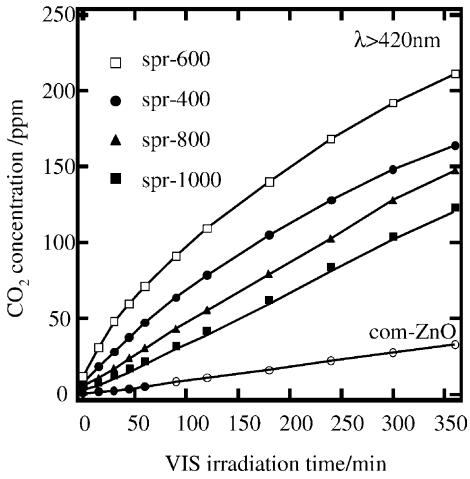

Fig. 8. Time-course of the CO_2 evolution during the Vis (>420 nm) photocatalytic decomposition of acetaldehyde on N-containing ZnO powders.

UV irradiation ($h\nu > 3.5$ eV), can be fulfilled even with the lower energy of Vis irradiation since a defect energy state is formed. However, the number of the electrons generated through Vis irradiation should be much lower than that with UV since much less Vis is absorbed (Fig. 3). Therefore, much lower Vis photocatalytic activity was observed than with UV. A similar model also explains the Vis photocatalysis on TiO_2 with oxygen vacancies [24]. In our case, oxygen vacancies should have existed when oxygen atoms were substituted with nitrogen atoms since nitrogen and oxygen have different valance states.

As mentioned, a higher nitrogen concentration should be expected since the Vis photocatalytic activity depends on the site-N concentration. However, more nitrogen doping can also make the sample more hydrophilic and thus, affect the sample stability. Zinc nitride is easily hydrolyzed by air moisture [9,25]. Further improvement of ZnO photocatalysis by increasing the nitrogen concentration without lowering stability is a goal for future research.

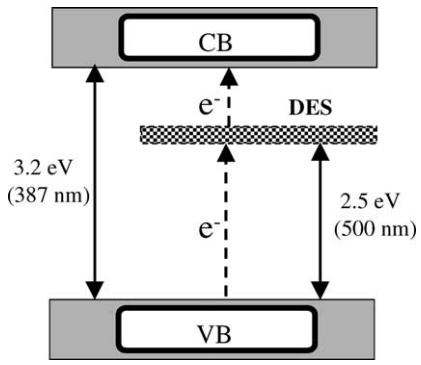

Fig. 9. Proposed energy-band structure model for the N-doping ZnO photocatalyst.

4. Conclusions

Spray pyrolysis was used to prepare N-containing ZnO powders with high surface area. The nitrogen atoms existed in two chemical forms. One was the site-N, meaning that these nitrogen atoms were doped into the sites of the ZnO crystal lattice by replacing oxygen atoms. The other was the residue-N that originated from the ZnO precursor residues. The total nitrogen concentration was controlled from 600 to 1400 ppm by changing the pyrolysis temperature. The site-N concentration ranged from 400 to 900 ppm. The N-containing ZnO powders could absorb part of the visible light, but did not change the UV absorption property of the ZnO. The photocatalytic performance of the N-containing ZnO powder was superior to that of a pure ZnO sample under visible light irradiation. However, nitrogen introduction had less effect on the UV photocatalytic activity of ZnO.

Acknowledgements

This research is part of the Millennium Project of “Search and Creation of a Catalyst for Removing Harmful Chemical Substances” from the Ministry of Education, Culture, Sports, Science and Technology (MEXT), Japan. We thank Dr. Y. Yajima for providing the elemental analysis results.

References

[1] T. Sehili, P. Boule, J. Lemaire, J. Photochem. Photobiol. A: Chem. 50 (1989) 103–116.
[2] J. Villasenor, P. Reyes, G. Pecchi, J. Chem. Technol. Biotechnol. 72 (1998) 105–110.
[3] M.D. Driessen, T.M. Miller, V.H. Grassian, J. Mol. Catal. A: Chem. 131 (1998) 149–156.
[4] M. Anpo, Catal. Surv. Jpn. 1 (1997) 169–179.
[5] M. Anpo, Pure Appl. Chem. 72 (2000) 1265–1270.
[6] R. Asahi, T. Morikawa, T. Ohwaki, K. Aoki, Y. Taga, Science 392 (2001) 269–271.
[7] T. Takada, G. Hitoki, A. Kasahara, D. Lu, J. Nomura, M. Hara, K. Domen, H. Kobayashi, Catalysts Catal. (Jpn.) 43 (6) (2001) 499–501.
[8] M. Jansen, H.P. Letschert, Nature 404 (2000) 980–982.
[9] M. Futsuhara, K. Yoshioka, O. Takai, Thin Solid Films 317 (1998) 322–325.
[10] X. Wang, S. Yang, J. Wang, M. Li, X. Jiang, G. Du, X. Liu, R.P.H. Chang, J. Cryst. Growth 226 (2001) 123–129.
[11] G.L. Messing, S. Zhang, G.V. Jayanthi, J. Am. Ceram. Soc. 76 (11) (1993) 2707–2726.
[12] S. Che, O. Sakurai, K. Shinozaki, N. Mizutani, J. Aerosol. Sci. 29 (3) (1998) 271–278.
[13] D. Li, N. Ichikuni, S. Shimazu, T. Uematsu, Appl. Catal. A: Gen. 172 (1998) 351–358.
[14] D. Li, N. Ichikuni, S. Shimazu, T. Uematsu, Appl. Catal. A: Gen. 180 (1999) 227–235.
[15] K.Y. Jung, Y.C. Kang, S.B. Park, J. Mater. Sci. Lett. 16 (1997) 1848–1849.
[16] R. Hoffmann, J. Chem. Phys. 40 (1964) 2474–2480.
[17] R. Marchand, F. Tessier, A. Le Sauze, N. Diot, Int. J. Inorg. Mater. 3 (2001) 1143–1146.
[18] H. Maki, N. Ichinose, I. Sakaguchi, N. Ohashi, H. Haneda, J. Tanaka, Key Eng. Mater. 216 (2002) 61–64.

[19] I. Sopyan, M. Watanabe, S. Murasawa, K. Hashimoto, A. Fujishima, J. Photochem. Photobiol. A: Chem. 98 (1996) 79–86.
[20] Y. Ohko, D.A. Tryk, K. Hashimoto, A. Fujishima, J. Phys. Chem. B 102 (1998) 2699–2704.
[21] M.R. Hoffmann, S.T. Martin, W. Choi, D.W. Bahnemann, Chem. Rev. 95 (1995) 69–96.
[22] L. Jing, Z. Xu, X. Sun, J. Shang, W. Cai, Appl. Surf. Sci. 180 (2001) 308–314.
[23] M.C. Markham, J.C. Kuriacose, J. DeMarco, C. Giaquinto, J. Phys. Chem. 66 (1962) 932–936.
[24] I. Nakamura, N. Negishi, S. Kutsuna, T. Ihara, S. Sugihara, K. Takeuchi, J. Mol. Catal. A: Chem. 161 (2000) 205–212.
[25] M. Futsuhara, K. Yoshioka, O. Takai, Thin Solid Films 322 (1998) 274–281.